

## Development of W-Reinforced Zr-Based Metallic Glass

Takeshi Terajima<sup>1,\*</sup>, Kazuhiro Nakata<sup>1</sup>, Hisamichi Kimura<sup>2</sup> and Akihisa Inoue<sup>3</sup>

<sup>1</sup>Joining and Welding Research Institute, Osaka University, Ibaraki 567-0047, Japan

<sup>2</sup>Institute for Material Research, Tohoku University, Sendai 980-8577, Japan

<sup>3</sup>Tohoku University, Sendai 980-8577, Japan

In order to improve the mechanical properties of  $Zr_{55}Al_{10}Ni_5Cu_{30}$  metallic glass, tungsten-reinforced  $Zr_{55}Al_{10}Ni_5Cu_{30}$  was developed. Tungsten particles with a diameter  $\phi = 100\ \mu\text{m}$  were uniformly distributed into the matrix, exhibiting good wettability with the  $Zr_{55}Al_{10}Ni_5Cu_{30}$  metallic glass matrix. Due to the extremely high melting temperature of tungsten, the tungsten particles coexisted with amorphous  $Zr_{55}Al_{10}Ni_5Cu_{30}$ , although a reaction layer of  $ZrW_2$  and a crystallized matrix formed to a certain extent depending on the sample. Nevertheless, the total amount of crystallization in both the matrix and the reaction phases remained small. As the volume fraction of W was increased from 0 to 8.7%, the plastic strain increased from 0 to 1.3%, and the fracture strength increased from 1480 to 1870 MPa. The coefficient of thermal expansion of monolithic  $Zr_{55}Al_{10}Ni_5Cu_{30}$  decreased from  $10.4 \times 10^{-6}\ \text{K}^{-1}$  to  $8.2 \times 10^{-6}\ \text{K}^{-1}$  in the case of the composite containing 30% W powder. [doi:10.2320/matertrans.ME200829]

(Received December 15, 2008; Accepted April 2, 2009; Published May 20, 2009)

**Keywords:** metallic glass, bulk amorphous alloy, composite, tungsten,  $Zr_{55}Al_{10}Ni_5Cu_{30}$

### 1. Introduction

Metallic glass exhibits many unique properties, such as high mechanical strength, small elastic coefficient, small solidification shrinkage, and high resistance to corrosion. As a result of these valuable properties, which cannot be found in crystalline metals, metallic glass has attracted the attention of many researchers, and shows potential for use in various industrial applications. Bulk metallic glass is generally produced by quenching a molten pre-alloy with the melt spinning method or the casting method. Some types of metallic glass, such as Mg-,<sup>1)</sup> Zr-,<sup>2,3)</sup> Fe-,<sup>4,5)</sup> Pd-,<sup>6)</sup> and Ni-based<sup>7)</sup> alloys, have a low critical cooling rate ( $R_c$ ), of which  $Pd_{42.5}Cu_{30}Ni_{7.5}P_{20}$  has the lowest  $R_c$  of 0.067 K/s.<sup>8)</sup> This strong glass-forming ability enables the production of bulk amorphous alloys with thickness of several centimeters.

One of the effective methods for improving and changing the mechanical properties of metallic glass is mixing reinforcements into the metallic glass matrix. Several types of composite materials comprising a metallic glass matrix have been developed so far.<sup>10–12)</sup> Although the powder metallurgy method<sup>9)</sup> is a somewhat complex process,<sup>13)</sup> it can produce satisfactory amorphous microstructures and larger bulk amorphous alloy composites than those fabricated by the casting method, at a temperature far below the liquidus temperature. The casting method has the advantage of easy utilization for mass production, while on the other hand, it contains the risk of inducing partial crystallization at the interface between the metallic glass matrix and the reinforcement. In addition, control of the wettability and dispersion of the reinforcements are highly important in the fabrication of composite materials. Almost all studies on metallic glass composite to date have focused on carbide reinforcements,<sup>10–12)</sup> such as ZrC, WC, and TiC, which have been mixed in advance with metallic glass pre-alloys by arc melting or produced by inducing an *in-situ* reaction of graphite with a Zr- or Ti-based metallic glass matrix. In

this study, a metal/metallic glass composite system (W/ $Zr_{55}Al_{10}Ni_5Cu_{30}$  composite) was studied.

### 2. Experimental

A pre-alloy ingot of  $Zr_{55}Al_{10}Ni_5Cu_{30}$  (in atom%) was prepared by arc-melting a mixture of pure Zr (99.9%), Al (99.9%), Ni (99.99%) and Cu (99.99%) metals in an oxygen-gettered argon atmosphere. The  $Zr_{55}Al_{10}Ni_5Cu_{30}$  pre-alloy was ground into particles with  $\phi = 150\ \mu\text{m}$ . The  $Zr_{55}Al_{10}Ni_5Cu_{30}$  powder was homogeneously mixed with W powder (average particle diameter  $\phi = 100\ \mu\text{m}$ , 99.9% purity). The volume fraction of W was controlled by adjusting a mixture ratio of W to  $Zr_{55}Al_{10}Ni_5Cu_{30}$  powder. In most cases, the intentional volume fraction was different from the actual volume fraction of the composite to some extent. The mixture was then pressed and shaped into a pellet in order to improve the efficiency of inductive heating. The pellet was melted in a quartz nozzle by inductive heating, after which the melt containing W powder was injected into a Cu mold, which contained an internal rod-shaped cavity with a hole with a diameter  $\phi = 3\ \text{mm}$  and a depth of 50 mm. However, with increasing W content, the quartz nozzle was often stopped up by W particle during the casting process. The temperature of the melt alloy was measured using a radiation thermometer, and was maintained at 1273 K. During the melting process, the  $Zr_{55}Al_{10}Ni_5Cu_{30}$  wet the W particles and simultaneously reacted with their surface.

The phases in the composites were identified by micro-focused X-ray diffraction (XRD) analysis using  $\text{Co K}\alpha$  radiation. The microstructure was examined with an optical microscope (OM), a scanning electron microscope (SEM), and an electron probe micro analyzer (EPMA). Furthermore, the thermal stability associated with the glass transition and crystallization was analyzed using a differential scanning calorimeter (DSC). Three specimens were prepared for 0, 3.1 and 8.7% W composites, respectively, and then the each specimen was cut into two for thermal mechanical analysis (TMA) and compressive test. Thermal expansion

\*Corresponding author, E-mail: terajima@jwri.osaka-u.ac.jp

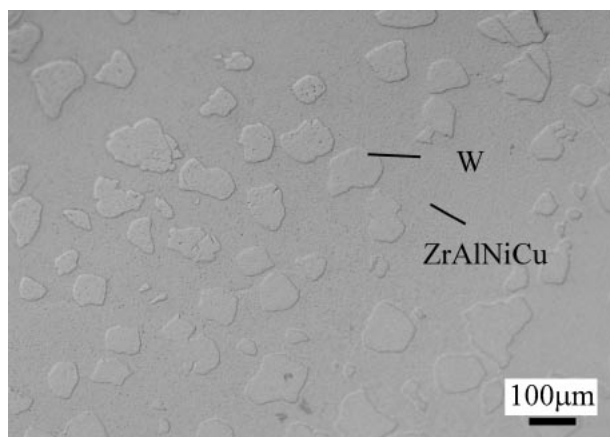


Fig. 1 Optical micrograph of the cross section of 20% W/Zr<sub>55</sub>Al<sub>10</sub>Ni<sub>5</sub>Cu<sub>30</sub> metallic glass composite.

was measured by TMA at a load of 1 N at a heating rate of 20 K/min. The diameter of the specimen was  $\phi = 3$  mm, and its length was 6 mm (aspect ratio 2). Compression tests were carried out at room temperature using an Instron universal testing system at a strain rate of  $5 \times 10^{-4} \text{ s}^{-1}$ . The compression test specimens were of the same shape as those used in the TMA.

### 3. Results and Discussion

Figure 1 shows the results obtained from the optical micrograph of the samples containing 20 vol% W. It is clear that the crystalline W particles embedded into the amorphous matrix are uniformly distributed. Neither pores nor voids appear over the entire cross section of the samples, indicating that a true bonding state exists at the interfaces between the amorphous matrix and the reinforcement particles. Figure 2 shows the micro-focused XRD patterns for the as-cast Zr<sub>55</sub>Al<sub>10</sub>Ni<sub>5</sub>Cu<sub>30</sub> metallic glass and the Zr<sub>55</sub>Al<sub>10</sub>Ni<sub>5</sub>Cu<sub>30</sub> metallic glass containing 3.1% and 8.7% W particles. It was confirmed that the composite material consists of the Zr<sub>55</sub>Al<sub>10</sub>Ni<sub>5</sub>Cu<sub>30</sub> glassy matrix, bcc-W, fcc-ZrW<sub>2</sub> and bct-Zr<sub>2</sub>Cu phases, and does not contain any other phases. ZrW<sub>2</sub> indicates the reaction layer between the Zr<sub>55</sub>Al<sub>10</sub>Ni<sub>5</sub>Cu<sub>30</sub> matrix and the W reinforcement particles. Furthermore, Fig. 3 shows DSC scans of the pure Zr<sub>55</sub>Al<sub>10</sub>Ni<sub>5</sub>Cu<sub>30</sub> and the W-reinforced composites for a heating rate of 20 K/min. An endothermic heat event characteristic of the glass transition is observed, followed by an exothermic heat release indicating the transformation from the metastable supercooling liquid state into the crystalline compounds.  $T_g$ ,  $T_x$ , and  $\Delta T$  of the composites are approximately 680, 761 and 81 K, respectively. Here,  $T_g$  and  $T_x$  are the onset temperature of their glass transition and crystallization events, respectively. The value  $\Delta T_x$  is defined as  $T_x - T_g$ , which is referred to as the supercooling liquid region. Based on the DSC scans, it was observed that the addition of W particles into the Zr<sub>55</sub>Al<sub>10</sub>Ni<sub>5</sub>Cu<sub>30</sub> matrix produced no discernible change in either  $T_g$  or  $T_x$ . Furthermore, the results of SEM imaging and element analyses at the interface between the W particles and the Zr<sub>55</sub>Al<sub>10</sub>Ni<sub>5</sub>Cu<sub>30</sub> matrix are shown in Fig. 4(a) and (b), respectively. A clearly contrasting reaction layer with a

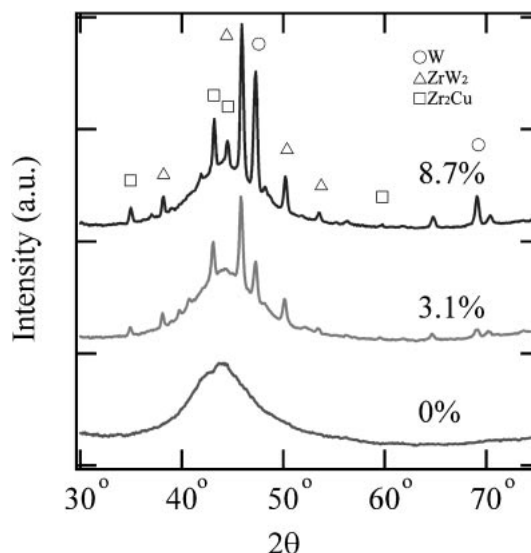


Fig. 2 Micro-focused X-ray diffraction patterns of the cross section of the W/Zr<sub>55</sub>Al<sub>10</sub>Ni<sub>5</sub>Cu<sub>30</sub> composite. Percentages shown are volume fractions of W reinforcement.

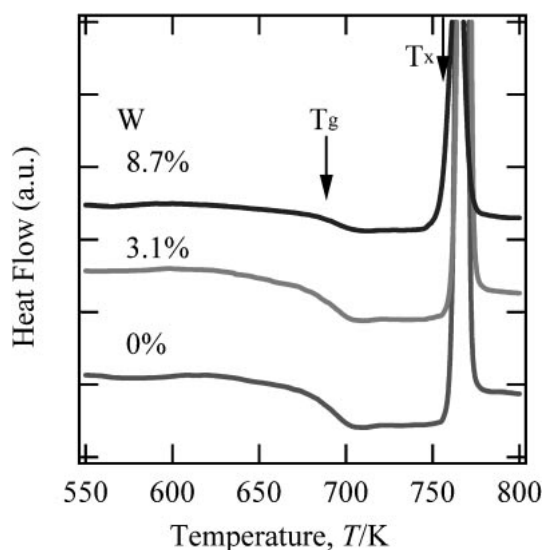


Fig. 3 Heat flow curves of W/Zr<sub>55</sub>Al<sub>10</sub>Ni<sub>5</sub>Cu<sub>30</sub> composites with different volume fractions of W powder ranging between 0 and 8.7% at a heating rate of 20 K/min.

thickness of 2  $\mu\text{m}$  was observed. Element analysis shows that the W particles coexist with the amorphous Zr<sub>55</sub>Al<sub>10</sub>Ni<sub>5</sub>Cu<sub>30</sub> matrix, although the abovementioned reaction layer formed between them, in which the atomic ratio of W/Zr was almost 2 and no other elements were detected. The reaction layer was characterized as consisting of ZrW<sub>2</sub> on the basis of the XRD and the element analysis results. Figure 5 shows the compression stress-strain curves of the monolithic Zr<sub>55</sub>Al<sub>10</sub>Ni<sub>5</sub>Cu<sub>30</sub> and the W-reinforced Zr<sub>55</sub>Al<sub>10</sub>Ni<sub>5</sub>Cu<sub>30</sub> at a strain rate of  $5 \times 10^{-4} \text{ s}^{-1}$ . As indicated, the behavior of the monolithic Zr<sub>55</sub>Al<sub>10</sub>Ni<sub>5</sub>Cu<sub>30</sub> is strictly elastic, without any macroscopic plastic deformation. However, the composites with different respective W content ratios exhibit improved compressive properties as compared to the monolithic Zr<sub>55</sub>Al<sub>10</sub>Ni<sub>5</sub>Cu<sub>30</sub>. With the increase in the content of the W

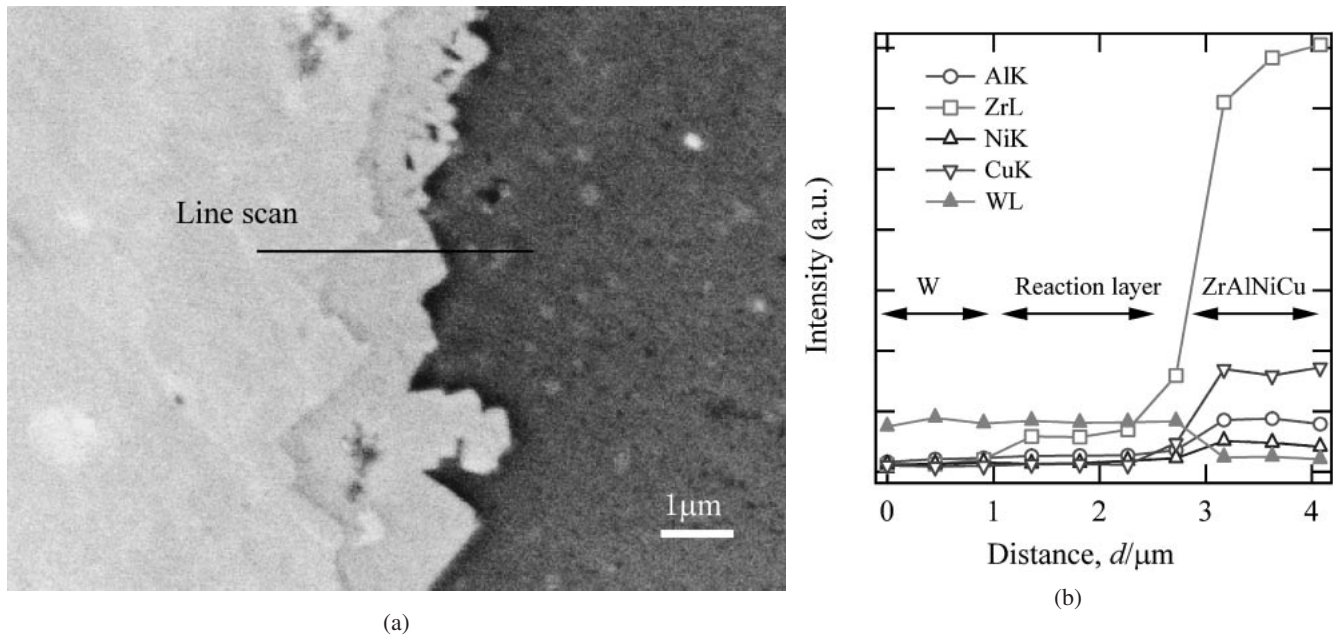


Fig. 4 (a) SEM micrograph and (b) element analysis results at the interface between a W particle and the  $Zr_{55}Al_{10}Ni_5Cu_{30}$  matrix.

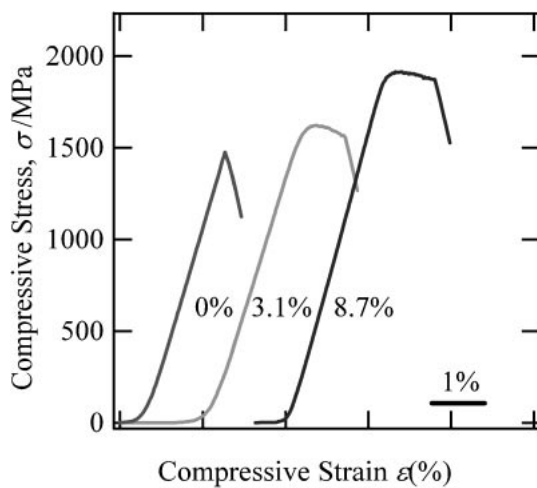


Fig. 5 Compression stress-strain curves for the monolithic  $Zr_{55}Al_{10}Ni_5Cu_{30}$  and the W-reinforced  $Zr_{55}Al_{10}Ni_5Cu_{30}$  for a strain rate of  $5 \times 10^{-4} s^{-1}$ .

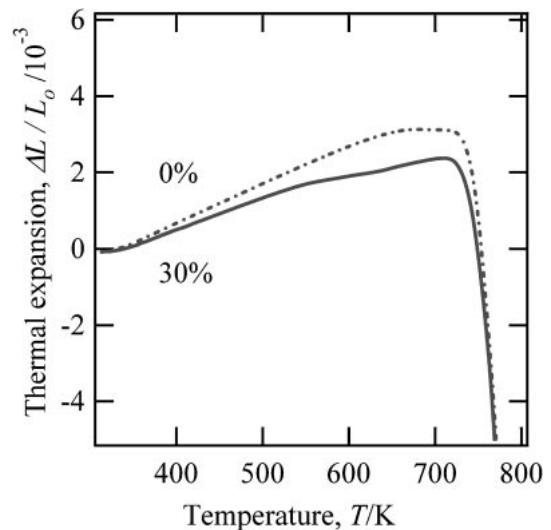


Fig. 6 Linear thermal expansion of the  $W/Zr_{55}Al_{10}Ni_5Cu_{30}$  composite as normalized with respect to the initial length at 300 K. Percentages shown are volume fractions of W reinforcement.

particles from 0 to 8.7%, the plastic strain increased from 0 to a maximum of 1.3%, the yield strength increased from 1480 to 1910 MPa, and the fracture strength increased from 1480 to 1870 MPa. The linear thermal expansion  $\Delta L/L_0$  is shown in Fig. 6 as normalized with respect to the initial length at 300 K. As the temperature increased from 300 to 700 K,  $\Delta L/L_0$  increased linearly, however, a drastic decrease was observed above 700 K. This corresponds to the decrease in viscosity at the transition from the glass state to the supercooling state. The coefficient of thermal expansion at 300 K was calculated from the inclination of  $\Delta L/L_0$  in the range between 300 and 400 K. In this regard, while the coefficient of thermal expansion of the monolithic  $Zr_{55}Al_{10}Ni_5Cu_{30}$  is  $10.4 \times 10^{-6} K^{-1}$ , it decreased to  $8.2 \times 10^{-6} K^{-1}$  in the case of the composite containing 30% W. This change of the coefficient of thermal expansion

is due to the fact that the coefficient of thermal expansion of W ( $4.5 \times 10^{-6} K^{-1}$ ) is approximately half of that of  $Zr_{55}Al_{10}Ni_5Cu_{30}$ .

$Zr_{55}Al_{10}Ni_5Cu_{30}$  has one of the lowest reported critical cooling rates, with the exception of Pd-based metallic glass. Also, the low liquidus temperature of the alloy allows the processing of the molten alloy at a relatively low temperature, and results in a minimal reaction between the matrix and the reinforcement. Furthermore, since a mixture of W and  $Zr_{55}Al_{10}Ni_5Cu_{30}$  particles was used as the pre-alloy in this experiment, a re-melting of the pre-alloy can be performed, and a reaction between the W particles and the  $Zr_{55}Al_{10}Ni_5Cu_{30}$  matrix can be induced at the same time, which serves to shorten the reaction time and suppress the reaction between the reinforcement and the matrix.

It is well known that the deformation mechanism in composites is different from that of monolithic metallic glass. This constraint leads to the generation of multiple shear bands parallel to the initial band. As a result of the generation of these bands, it is reasonable to assume that the plastic strain performance is enhanced in comparison to that of the monolithic  $Zr_{55}Al_{10}Ni_5Cu_{30}$ , as shown in Fig. 5. The improvement of the compressive stress is due to the restraint of slipping imposed on each shear plane by the W particles. This behavior also enhances the fracture toughness of the composite.

As can be expected, the coefficient of thermal expansion of the composite decreased since the coefficient of thermal expansion of W is about half of that of the monolithic  $Zr_{55}Al_{10}Ni_5Cu_{30}$ . It is well known that the thermal expansion coefficient of composites at 300 K is calculated from the rule of mixtures ( $\alpha = \sum \alpha_i V_i$ ), where  $i$  represents the reinforcements,  $\alpha$  is the coefficient of thermal expansion, and  $V$  is the volume fraction. The calculated value of the composite containing 30% W is  $8.6 \times 10^{-6} K^{-1}$ . This is in good agreement with the experimental value of  $8.2 \times 10^{-6} K^{-1}$ , which can be explained by the fact that the rule of mixtures is only valid for samples which are free of voids and internal stress.

#### 4. Conclusion

Tungsten-reinforced  $Zr_{55}Al_{10}Ni_5Cu_{30}$  metallic glass composite was successfully fabricated by applying the injection cast method. W particles were homogeneously dispersed into the amorphous  $Zr_{55}Al_{10}Ni_5Cu_{30}$  matrix. When the W volume fraction was increased from 0 to 8.7%, the plastic strain increased from 0 to 1.3%, and the fracture strength increased from 1480 to 1870 MPa. The coefficient of thermal expansion decreased from  $10.4 \times 10^{-6} K^{-1}$  to  $8.2 \times 10^{-6} K^{-1}$  in the

case of the composite containing 30% W powder. This result is in good agreement with the calculated value of  $8.6 \times 10^{-6} K^{-1}$ , which is based on the rule of mixtures for composite materials.

#### Acknowledgement

This work was supported by a Grant-in-Aid for the Cooperative Research Project of the Nationwide Joint-Use Research Institutes on the Development Base of Joining Technology for New Metallic Glasses and Inorganic Materials from The Ministry of Education, Culture, Sports, Science and Technology, Japan.

#### REFERENCES

- 1) M. Calin, J. Eckert and L. Schultz: *Scr. Mater.* **48** (2003) 653–658.
- 2) J. Saida, A. Deny, H. Setyawan, H. Kato and A. Inoue: *Appl. Phys. Lett.* **87** (2005) 151907 1-3.
- 3) W. H. Wang and H. Y. Bai: *Mater. Lett.* **44** (2000) 59–63.
- 4) J. Das, M. B. Tang, K. B. Kim, R. Theissma, F. Baler, W. H. Wang and J. Eckert: *Phys. Rev. Lett.* **94** (2005) 205501 1-4.
- 5) K. B. Kim, J. Das, F. Baier, M. B. Tang, W. H. Wang and J. Eckert: *Appl. Phys. Lett.* **88** (2006) 051911 1-3.
- 6) H. Kato and A. Inoue: *Mater. Trans. JIM* **38** (1997) 793–800.
- 7) J. Li, L. Wang, H. F. Zhang, Z. Q. Hu and H. Cai: *Mater. Lett.* **61** (2007) 2217–2221.
- 8) D. G. Pan, H. F. Zhang, A. M. Wang and Z. Q. Hu: *Appl. Phys. Lett.* **89** (2006) 261904 1-3.
- 9) G. Xie, D. V. Louzguine-Luzgin, F. Wakai, H. Kimura and A. Inoue: *Mater. Sci. Eng. B* **148** (2008) 77–81.
- 10) T. Hirano, H. Kato, A. Matsuo, Y. Kawamura and A. Inoue: *Mater. Trans. JIM* **41** (2000) 1454–1459.
- 11) H. Fu, H. Zhang, H. Wang, Q. Zhang and Z. Hu: *Scr. Mater.* **52** (2005) 669–673.
- 12) Y. F. Sun, C. H. Shek, S. K. Guan, B. C. Wei and J. Y. Geng: *Mater. Sci. Eng. A* **435–436** (2006) 132–138.
- 13) A. Inoue: *Mater. Trans. JIM* **36** (1995) 866–875.